

---

This is an electronic reprint of the original article.  
This reprint may differ from the original in pagination and typographic detail.

Heilmann, Rebecca; Arjas, Kristian; Törmä, Päivi  
**Lasing in nanoparticle arrays with complex unit cells**

*Published in:*  
Nanophotonics X

*DOI:*  
[10.1117/12.3015176](https://doi.org/10.1117/12.3015176)

Published: 01/01/2024

*Document Version*  
Publisher's PDF, also known as Version of record

*Please cite the original version:*  
Heilmann, R., Arjas, K., & Törmä, P. (2024). Lasing in nanoparticle arrays with complex unit cells. In D. L. Andrews, A. J. Bain, & A. Ambrosio (Eds.), *Nanophotonics X* (pp. 1-7). Article 129910H (Proceedings of SPIE - The International Society for Optical Engineering; Vol. 12991). SPIE. <https://doi.org/10.1117/12.3015176>

---

This material is protected by copyright and other intellectual property rights, and duplication or sale of all or part of any of the repository collections is not permitted, except that material may be duplicated by you for your research use or educational purposes in electronic or print form. You must obtain permission for any other use. Electronic or print copies may not be offered, whether for sale or otherwise to anyone who is not an authorised user.

# Lasing in nanoparticle arrays with complex unit cells

Rebecca Heilmann<sup>a</sup>, Kristian Arjas<sup>a</sup>, and Päivi Törmä<sup>a</sup>

<sup>a</sup>Department of Applied Physics, Aalto University School of Science, P.O. Box 15100, Aalto, FI-00076, Finland

## ABSTRACT

In this work, we study lasing in plasmonic nanoparticle arrays with complex structures. Complex structures can be formed by unit cells that contain more than one particle or by creating supercells i.e. giant unit cells, which contain tens of particles. Here, we study lasing in supercell arrays which are based on a square array geometry. The supercell is created by leaving certain lattice sites empty, creating an aperiodic pattern. This supercell is repeated to form an array. We calculate the band structures of the arrays by combining the structure factors of the lattice geometries with an empty lattice approximation. We show that by leaving certain lattice sites empty, some of the destructive interference is removed, leading to additional dispersive branches. This provides new band edges that support lasing. We experimentally demonstrate lasing in such supercell arrays which show interesting lasing emission patterns and multimode lasing.

**Keywords:** plasmonics, lasing, surface lattice resonance

## 1. INTRODUCTION

Arrays of metallic nanoparticles host surface lattice resonances (SLRs) which are hybrid modes of the diffracted orders of the lattice and the plasmonic resonances of the individual nanoparticles. These SLRs provide narrow linewidths and at the same time high optical field confinements.<sup>1-7</sup> Combined with a gain medium, such as organic dye molecules, such plasmonic nanoparticle arrays are an excellent platform to study light-matter interaction, including strong coupling, Bose-Einstein condensation, and lasing.<sup>8-13</sup>

The resonances of plasmonic nanoparticle arrays are controlled by the lattice geometry and lattice period, where lasing has been realized in the high symmetry points of the arrays, for example in the  $\Gamma$ -,  $K$ -, and  $M$ -points in different lattice geometries.<sup>14-18</sup> The high symmetry points open up band gaps, which in turn provide feedback for lasing phenomena.

Complex array structures can be created by adding or removing particles in the unit cell. Arrays with more than one particle in the unit cell have been utilized to realize lasing in bound states in continuum.<sup>19,20</sup> Superarrays, i.e. arrays arranged in patches provide multiple band edges as the SLRs of the individual array patches couple to the Bragg modes of the superarrays. Multimode lasing has been shown in such superarrays.<sup>21,22</sup> In addition, multimode lasing was observed in supercell arrays.<sup>23</sup> Such supercell arrays are created by removing particles in an array geometry leaving certain lattice sites empty. By removing the particles, larger aperiodic patterns can be created, which form a supercell. These supercells are then arranged periodically into an array. Removing particles leads to new dispersive modes as part of the destructive interference is removed, which in turn provides new band edges where lasing can occur.

Here, we study a supercell array based on a square array geometry. The square array period is tuned over a wide range of periods, while the supercell array structure stays the same. The presence of the additional dispersive modes due to the supercell enable us to study lasing phenomena far away from the  $\Gamma$ -point defined

---

Further author information: (Send correspondence to P.T. or R.H.)

E-mail (P.T.): paivi.torma@aalto.fi,

E-mail (R.H.): rebecca.heilmann@aalto.fi

by the period of the underlying square lattice. For this, we combine the arrays with organic dye molecules as a gain medium for lasing. Although the  $\Gamma$ -point that stems from the square array period does not overlap with the emission spectrum of the dye molecules, we observe lasing in the additional modes caused by the supercell structure. We calculate  $k$ -space images using the empty lattice approximation based on the structure factor of the supercell array for different square array periods and compare them to experimentally recorded full  $k$ -space images to identify the lasing modes.

## 2. RESULTS

The complex unit cell nanoparticle arrays are based on a square array geometry with a period  $p$ . By removing particles at specific positions in the square array, we create an aperiodic pattern which in turn creates a supercell with a period  $P$ . The supercell pattern studied here is based on a 2D Thue-Morse sequence<sup>24,25</sup> that creates a supercell period of  $P = 32p$  as shown in Fig. 1 a). This supercell is repeated periodically, to form an array.

We study the array structure theoretically by calculating the structure factor and the empty lattice approximation as discussed in detail in Reference [23]. The structure factor is a measure of the scattering properties of an array of scatterers and contains information on constructive interference for every wave vector  $k$ . The structure factor of the supercell array considered is shown in Fig. 1 b). The bright yellow spot in the center of the Brillouin Zone (indicated by the blue dashed line) stems from the period of the underlying square lattice period  $2\pi/p$  and corresponds to the  $\Gamma$ -point of the lattice. There are additional, red, spots visible in other parts of the Brillouin Zone, albeit of less intensity. Due to the supercell period  $P$  the original Brillouin Zone is divided into smaller Brillouin Zones  $2\pi/P$  and constructive interference is allowed in some of these smaller Brillouin Zones caused by the missing particles.

The empty lattice approximation considers the free space photon dispersion  $\|\mathbf{k}\| = \sqrt{k_x^2 + k_y^2} = \frac{nE}{\hbar c}$ , where  $\|\mathbf{k}\|$  is the in-plane wave vector,  $n$  the refractive index of the medium,  $E$  the photon energy,  $\hbar$  Planck's constant, and  $c$  the vacuum speed of light. The free photon dispersion corresponds to a conical surface in  $k_x, k_y, E$ -space and is often referred to as a light cone. The simplest approximation of the photonic band structure is obtained by taking the convolution of the structure factor and the light cones. In practice, this corresponds to placing light cones in  $k$ -space and weighing them by the structure factor at their tip. To study the dispersions the band structure is calculated for multiple periods as shown in Fig. 1 c-d). The  $\Gamma$ -point of the underlying square lattice is at an energy  $E = \frac{2\pi\hbar c}{np}$  and is not visible in Fig. 1 c) and d) as it is at a higher energy for these periods. For  $p = 580$  nm, the  $\Gamma$ -point is located at an energy of 1.406 eV as shown in Fig. 1 e). In addition to the dispersion branches that stem from the underlying square lattice, additional weaker features emerge due to the removed particles. By changing the period of the underlying square lattice, the dispersion can be shifted to different energies which allows for probing different modes experimentally.

Next, we study experimentally lasing in such supercell arrays. We fabricate nanoparticle arrays with an edge length of 130  $\mu\text{m}$  with electron beam lithography. The arrays consist of cylindrical gold nanoparticles with a diameter of 110 nm and a height of 50 nm. The period  $p$  of the underlying square lattice is varied from 320 to 580 nm. We combine the arrays with a solution of organic emitters (IR 140) dissolved in a 1:2 mixture of benzyl alcohol and dimethyl sulfoxide to match the refractive index  $n = 1.52$  of the substrate. The concentration of the dye molecules was 10 mM. We optically pump the system with a laser pulse of 800 nm center wavelength and 1kHz repetition rate. For increasing pump intensity, different lasing peaks are observed for different periods of the underlying square lattice as shown in Fig. 2. For a period of  $p = 580$  nm we observe one lasing peak at an energy of  $E = 1.404$  eV, which corresponds to lasing in the  $\Gamma$ -point of the underlying square lattice as the threshold curve indicates in Fig. 2 a) as well as the spectrometer data in Fig. 2 b). For arrays with an underlying square array period, where the  $\Gamma$ -point does not overlap with the emission spectrum of the gain medium, we indeed observe lasing in the new modes that stem from the supercell structure. Specifically, there are two lasing peaks for a square lattice period of  $p = 500$  nm at an energy of  $E = 1.408$  eV (see Figs. 2 d,e)), and, similarly, for a period of  $p = 320$  nm we observe four lasing peaks at an energy of  $E = 1.399$  eV (see Figs. 2 g,h).

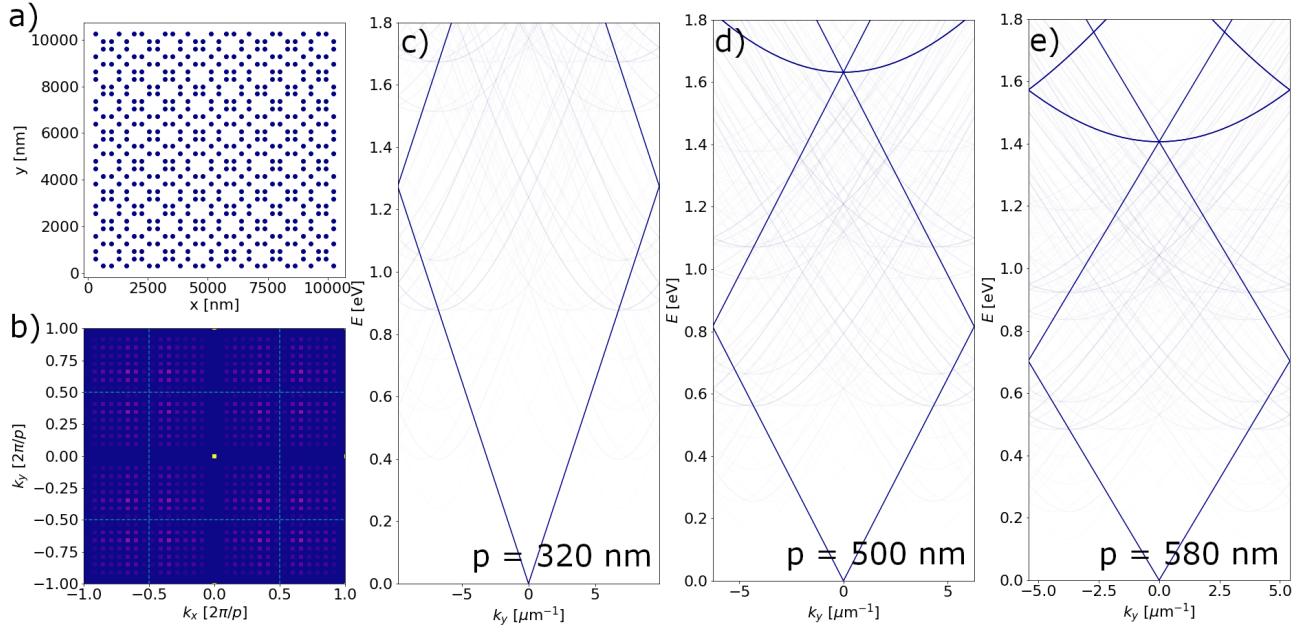


Figure 1. Schematic of the supercell array. a) Supercell structure of the particle positions, b) structure factor calculated from supercell, the dashed blue lines indicate the Brillouin Zone caused by the underlying square lattice period  $p$ . The intensity of the allowed constructive interference is indicated by the color scale, where low to high intensity is indicated from blue to yellow. c-d) Calculated dispersions based on the empty lattice approximation of supercell arrays with different square lattice periods  $p = 320, 500,$  and  $580$  nm. The refractive index of the medium is  $n = 1.52$ .

In addition to the emission spectra, we measured full momentum space images of the lasing emission for arrays with different underlying square lattice periods  $p$  as shown in Fig. 2 c,f,i) for  $p = 580$  nm,  $500$  nm, and  $320$  nm, respectively. These images only contain information on the angular distribution of the lasing emission from the arrays, however, they do not contain spectral information of the peaks, as only a long pass filter with a cut-off wavelength of  $850$  nm was used. The circle in the momentum space images is defined by the numerical aperture ( $NA = 0.3$ ) of the objective and the two circles in the center visible in some of the measurements (e.g. for  $p = 320$  nm) are reflections of the pump beam at the sample substrate. Although most of the pump is filtered out with the long pass filter, the tail of the pump is still visible, especially if the emission from the array is of similar intensity such as in Fig. 2 i).

The spectrometer only records the data along  $\theta_x = 0$ , hence we were not able to record the spectra of peaks that are not along  $\theta_x = 0$ . However, from Figs. 2 f) and i), it is evident, that there are more points, from which the array emits light. For instance in Fig. 2 f) ( $p = 500$  nm), there are additional peaks at  $\theta_y = \pm 13.4^\circ$  and  $\theta_x = \pm 3.4^\circ$ . Similarly, weaker peaks are visible at  $\theta_x = \pm 13.4^\circ$  and  $\theta_y = \pm 3.4^\circ$ . For the array with the period  $p = 320$  nm in Fig. 2 i), the  $k$ -space emission pattern becomes more complex: for instance, there are four additional peaks for combinations of  $\theta_{x,y} \pm 2.6^\circ$ , as well as peaks at  $\theta_x = \pm 10.5^\circ$  and  $\theta_y = \pm 4.1^\circ$ . In addition, a cross pattern of weak lines is visible, which corresponds to emission from the SLRs of the array.

Figure 3 shows the full  $k$ -space images of arrays that either did not show lasing or showed lasing in modes that are not along  $\theta_x = 0$ . To understand the nature of the modes, we compare the measured  $k$ -space image with theoretically calculated  $k$ -space images based on the empty lattice approximation. Since the empty lattice approximation only gives information on the dispersions of the array structure and not on the modes that are lasing, we benchmark the empty lattice approximation with an array that did not show lasing but showed emission from the SLRs in Figure 3 a) for an array with a period of  $p = 540$  nm. The the experimental  $k$ -space data is shown in the most left image, the simulated  $k$ -space image is shown in the most right image and an overlay of

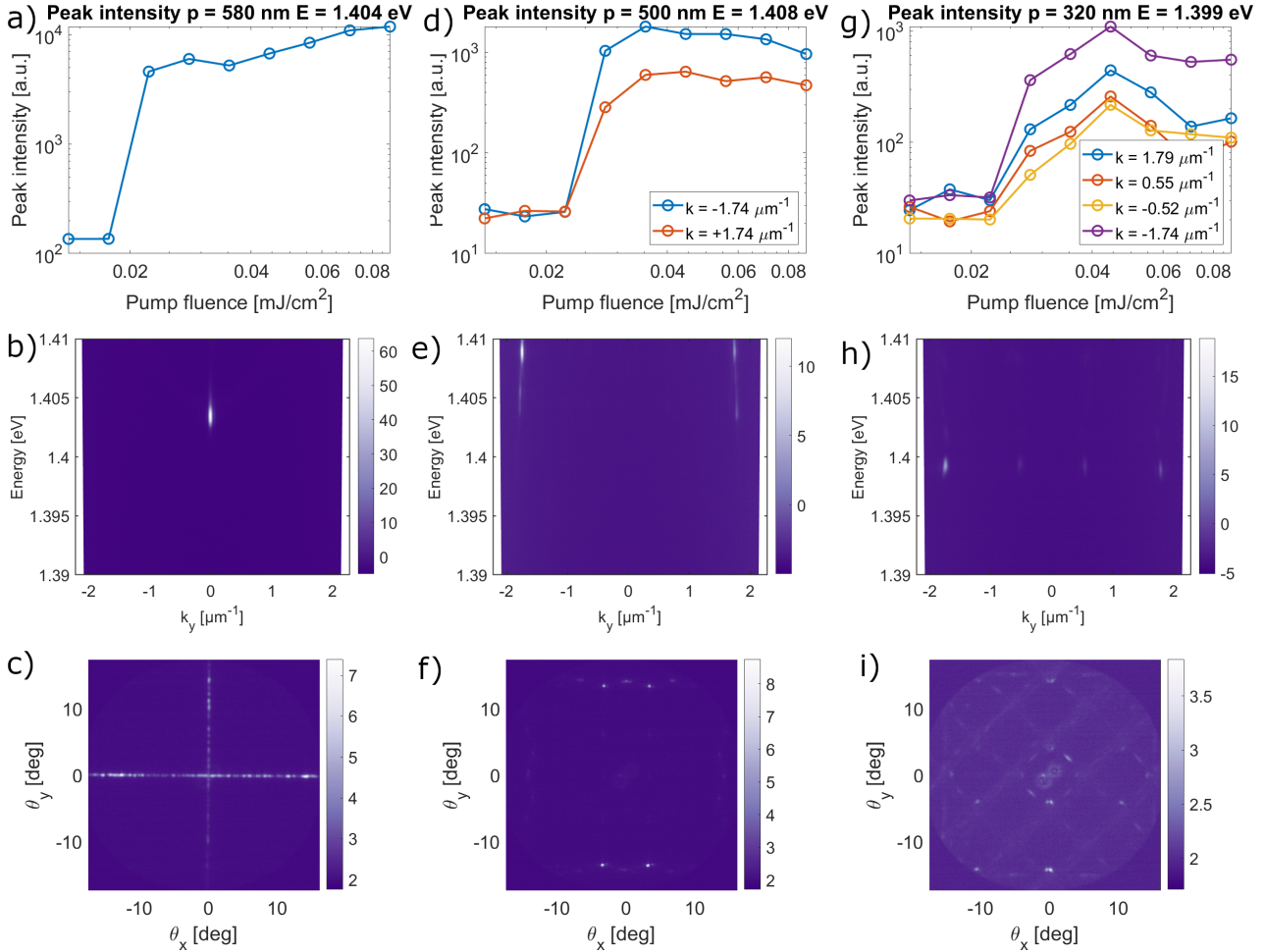


Figure 2. Lasing in supercell arrays with different periods of the underlying square lattice. Lasing in a supercell array with a period  $p=580$  nm is shown in a) threshold curve, b) spectrometer data, and c) full  $k$ -space image. The threshold curve, spectrometer data, and full  $k$ -space image for lasing in an array with a period  $p = 500$  nm are shown in d), e), and f), respectively. Corresponding images for lasing in an array with a period  $p = 320$  nm are shown in g), h), and i). The spectrometer and full  $k$ -space images are shown for a pump fluence of  $0.0444$  mJ/cm<sup>2</sup>.

experimental, and simulated data is shown in the central image and shows excellent agreement. In the case of an array with  $p = 420$  nm (see Fig. 3 b)), we experimentally observe several sets of four peaks close to each other, where the sets closer to the center have the highest intensity. As none of these peaks is along  $\theta_x = 0$ , we cannot study their spectral properties in the spectrometer. However, based on the simulations we find that these sets of four peaks stem from several SLRs that overlap, creating a band gap that provides a ground state for lasing. In Fig. 3 c), we show an array with a period of  $p = 380$  nm, which again mainly shows emission from the SLRs, however, this pattern appears much more complex than that in Fig. 3 a). We are able to reproduce the octagonal shape with the empty lattice approximation, enabling us to identify the SLRs from which the emission stems.

### 3. CONCLUSIONS

We experimentally studied lasing in supercell arrays and found that arrays showed lasing, although the period of the underlying square lattice is far away from the  $\Gamma$ -point. The supercell structure of the arrays allows for new modes that provide feedback for lasing, even off- $\Gamma$ -point as long as they overlap with the emission spectrum of

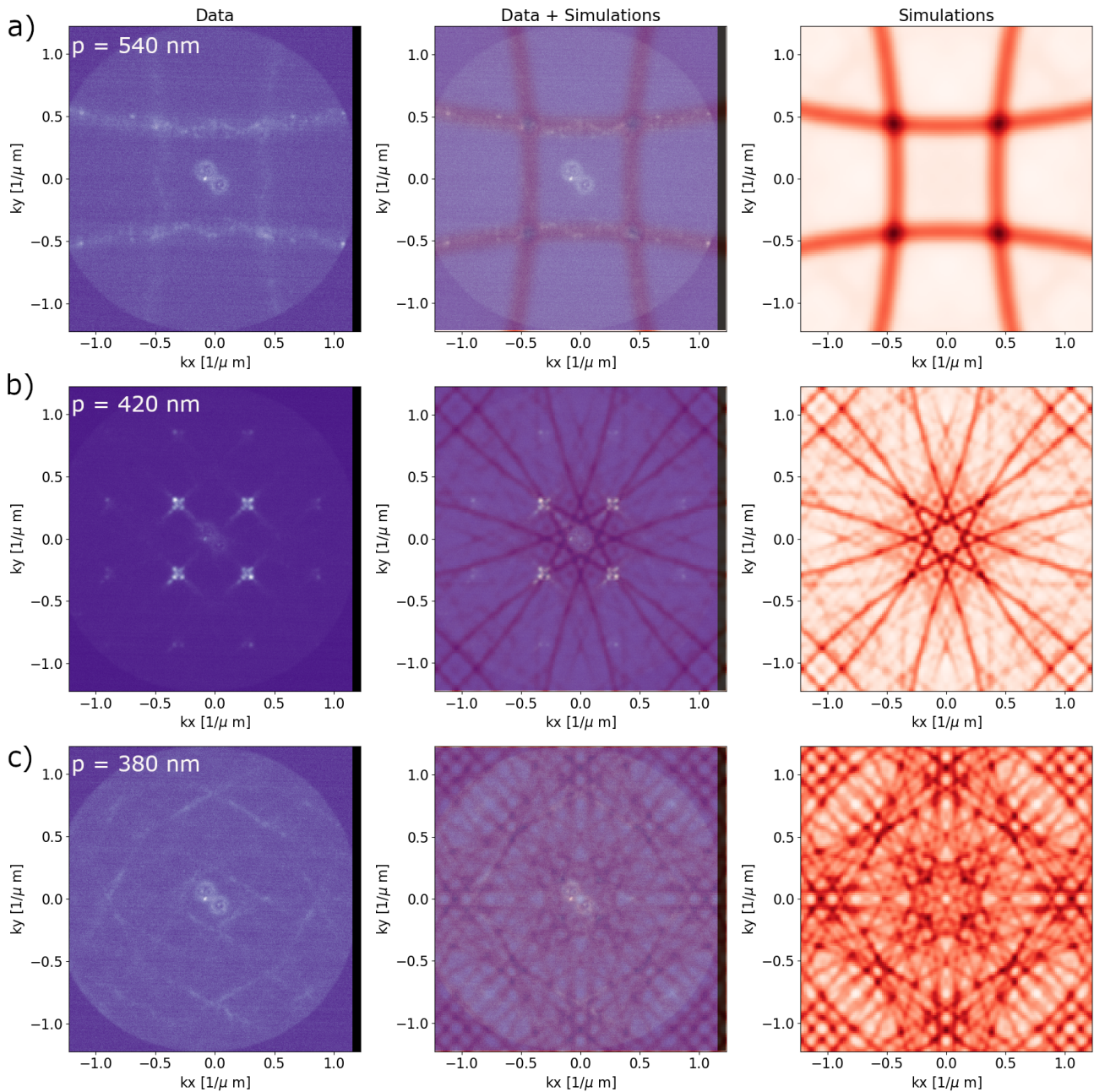


Figure 3. Comparisons with the theoretical predictions for systems with three different periods. The first row a) corresponds to a  $p = 540$  nm which did not show lasing in the experiments. The light cones are modelled as gaussians with  $\sigma = 4 \times 10^{-3}$  below lasing threshold (a) and  $\sigma = 4 \times 10^{-4}$  above lasing threshold (b and c). The second row b) shows measurements from  $p = 420$  nm where strong lasing peaks are observed. The lasing peaks can be seen at crossings of a few of the strongest light cones. The third row c) corresponds to  $p = 380$  nm where the octagonal shape observed in the emission is reproduced by the light cones. It should be noted, that the strongest light cones are ignored in this plot to highlight this shape. The experimental  $k$ -space data (first column) are shown for a pump fluence of  $0.0444$  mJ/cm<sup>2</sup>.

the gain medium. In addition, we observed simultaneous lasing from different angles, as well as complex emission patterns in full  $k$ -space. We simulated the dispersions in  $k$ -space based on the empty lattice approximation and found an excellent agreement with the measured  $k$ -space emission patterns, enabling the identification of the modes.

As the empty lattice approximation does not contain any information on the plasmonic nature of the mode, predictions on which modes will be lasing cannot be made solely based on this method. Although there appears to be a connection between the lasing modes and the strength of the modes in the empty lattice approximation,<sup>23</sup> some of the modes emitting were surprising. For instance, in Fig 3 c), the strongest light cones in the simulations were ignored, to make the octagonal shape visible.

Nanoparticle arrays with complex structures offer a new degree of freedom in designing the band structure of nanoparticle arrays. Supercell arrays specifically provide new possibilities for dispersion engineering due to their rich band structure caused by the arrangement of the particles within the supercell.

## ACKNOWLEDGMENTS

The work is part of the Research Council of Finland Flagship Programme, Photonics Research and Innovation (PREIN), decision number 346529, Aalto University, and the Vilho, Yrjö and Kalle Väisälä Foundation. Part of the research was performed at the OtaNano Nanofab cleanroom (Micronova Nanofabrication Centre), supported by Aalto University. We acknowledge the computational resources provided by the Aalto Science-IT project. R.H. acknowledges financial support by the Finnish Foundation for Technology Promotion.

## REFERENCES

- [1] Kravets, V., Schedin, F., and Grigorenko, A., “Extremely narrow plasmon resonances based on diffraction coupling of localized plasmons in arrays of metallic nanoparticles,” *Physical Review Letters* **101**(8), 087403 (2008).
- [2] Chu, Y., Schonbrun, E., Yang, T., and Crozier, K. B., “Experimental observation of narrow surface plasmon resonances in gold nanoparticle arrays,” *Applied Physics Letters* **93**(18), 181108 (2008).
- [3] Auguié, B. and Barnes, W. L., “Collective resonances in gold nanoparticle arrays,” *Physical Review Letters* **101**(14), 143902 (2008).
- [4] Giannini, V., Fernández-Domínguez, A. I., Heck, S. C., and Maier, S. A., “Plasmonic nanoantennas: fundamentals and their use in controlling the radiative properties of nanoemitters,” *Chemical reviews* **111**(6), 3888–3912 (2011).
- [5] Rodriguez, S. R. K., Abass, A., Maes, B., Janssen, O. T., Vecchi, G., and Rivas, J. G., “Coupling bright and dark plasmonic lattice resonances,” *Physical Review X* **1**(2), 021019 (2011).
- [6] Humphrey, A. D. and Barnes, W. L., “Plasmonic surface lattice resonances on arrays of different lattice symmetry,” *Physical Review B* **90**(7), 075404 (2014).
- [7] Ross, M. B., Mirkin, C. A., and Schatz, G. C., “Optical properties of one-, two-, and three-dimensional arrays of plasmonic nanostructures,” *The journal of physical chemistry C* **120**(2), 816–830 (2016).
- [8] Väkeväinen, A. I., Moerland, R., Rekola, H., Eskelinen, A.-P., Martikainen, J.-P., Kim, D.-H., and Törmä, P., “Plasmonic surface lattice resonances at the strong coupling regime,” *Nano Letters* **14**(4), 1721–1727 (2014).
- [9] Bozhevolnyi, S. I., Martin-Moreno, L., and Garcia-Vidal, F., [*Quantum Plasmonics*], Springer (2017).
- [10] Hakala, T. K., Moilanen, A. J., Väkeväinen, A. I., Guo, R., Martikainen, J.-P., Daskalakis, K. S., Rekola, H. T., Julku, A., and Törmä, P., “Bose–einstein condensation in a plasmonic lattice,” *Nature Physics* **14**(7), 739–744 (2018).
- [11] De Giorgi, M., Ramezani, M., Todisco, F., Halpin, A., Caputo, D., Fieramosca, A., Gomez-Rivas, J., and Sanvitto, D., “Interaction and coherence of a plasmon–exciton polariton condensate,” *ACS Photonics* **5**(9), 3666–3672 (2018).

- [12] Wang, W., Ramezani, M., Väkeväinen, A. I., Törmä, P., Rivas, J. G., and Odom, T. W., “The rich photonic world of plasmonic nanoparticle arrays,” *Materials Today* **21**(3), 303–314 (2018).
- [13] Väkeväinen, A. I., Moilanen, A. J., Nečada, M., Hakala, T. K., Daskalakis, K. S., and Törmä, P., “Sub-picosecond thermalization dynamics in condensation of strongly coupled lattice plasmons,” *Nature Communications* **11**(1), 3139 (2020).
- [14] Zhou, W., Dridi, M., Suh, J. Y., Kim, C. H., Co, D. T., Wasielewski, M. R., Schatz, G. C., and Odom, T. W., “Lasing action in strongly coupled plasmonic nanocavity arrays,” *Nature Nanotechnology* **8**(7), 506–511 (2013).
- [15] Yang, A., Hoang, T. B., Dridi, M., Deeb, C., Mikkelsen, M. H., Schatz, G. C., and Odom, T. W., “Real-time tunable lasing from plasmonic nanocavity arrays,” *Nature Communications* **6**(1), 6939 (2015).
- [16] Ramezani, M., Halpin, A., Fernández-Domínguez, A. I., Feist, J., Rodríguez, S. R.-K., Garcia-Vidal, F. J., and Rivas, J. G., “Plasmon-exciton-polariton lasing,” *Optica* **4**(1), 31–37 (2017).
- [17] Guo, R., Nečada, M., Hakala, T. K., Väkeväinen, A. I., and Törmä, P., “Lasing at k points of a honeycomb plasmonic lattice,” *Physical Review Letters* **122**(1), 013901 (2019).
- [18] Juarez, X. G., Li, R., Guan, J., Reese, T., Schaller, R. D., and Odom, T. W., “M-point lasing in hexagonal and honeycomb plasmonic lattices,” *ACS Photonics* **9**(1), 52–58 (2022).
- [19] Heilmann, R., Salerno, G., Cuerda, J., Hakala, T. K., and Törmä, P., “Quasi-BIC mode lasing in a quadrumer plasmonic lattice,” *ACS Photonics* **9**(1), 224–232 (2022).
- [20] Salerno, G., Heilmann, R., Arjas, K., Aronen, K., Martikainen, J.-P., and Törmä, P., “Loss-driven topological transitions in lasing,” *Physical Review Letters* **129**(17), 173901 (2022).
- [21] Wang, D., Yang, A., Wang, W., Hua, Y., Schaller, R. D., Schatz, G. C., and Odom, T. W., “Band-edge engineering for controlled multi-modal nanolasing in plasmonic superlattices,” *Nature Nanotechnology* **12**(9), 889–894 (2017).
- [22] Wang, D., Guan, J., Hu, J., Bourgeois, M. R., and Odom, T. W., “Manipulating light–matter interactions in plasmonic nanoparticle lattices,” *Accounts of Chemical Research* **52**(11), 2997–3007 (2019).
- [23] Heilmann, R., Arjas, K., Hakala, T. K., and Törmä, P., “Multimode lasing in supercell plasmonic nanoparticle arrays,” *ACS Photonics* **10**(11), 3955–3962 (2023).
- [24] Dal Negro, L. and Boriskina, S. V., “Deterministic aperiodic nanostructures for photonics and plasmonics applications,” *Laser & Photonics Reviews* **6**(2), 178–218 (2012).
- [25] Schokker, A. H. and Koenderink, A. F., “Lasing in quasi-periodic and aperiodic plasmon lattices,” *Optica* **3**(7), 686–693 (2016).